Molecular Crystals and Liquid Crystals

ISSN: 1542-1406 (Print) 1563-5287 (Online) Journal homepage: http://www.tandfonline.com/loi/gmcl20

Structural and thermo-optic studies on linear double hydrogen bonded ferroelectric liquid crystal homologous series

T. Mahalingam, T. Venkatachalam, R. Jayaprakasam & V. N. Vijayakumar

To cite this article: T. Mahalingam, T. Venkatachalam, R. Jayaprakasam & V. N. Vijayakumar (2016) Structural and thermo-optic studies on linear double hydrogen bonded ferroelectric liquid crystal homologous series, Molecular Crystals and Liquid Crystals, 641:1, 10-24, DOI: 10.1080/15421406.2016.1235927

To link to this article: http://dx.doi.org/10.1080/15421406.2016.1235927

MOLECULAR CRYSTALS AND LIQUID CRYSTALS
2016, VOL. 641, 10–24
http://dx.doi.org/10.1080/15421406.2016.1235927

Taylor & Francis
Taylor & Francis Group

Structural and thermo-optic studies on linear double hydrogen bonded ferroelectric liquid crystal homologous series

T. Mahalingam[a], T. Venkatachalam[b], R. Jayaprakasam[c], and V. N. Vijayakumar[d]

[a]Department of Physics, Kathir College of Engineering, Coimbatore, India; [b]Department of Physics, Coimbatore Institute of Technology, Coimbatore, India; [c]Department of Chemistry, Bannari Amman Institute of Technology, Sathyamangalam, India; [d]Department of Physics, Condensed Matter Research Laboratory (CMRL), Bannari Amman Institute of Technology, Sathyamangalam, India

ABSTRACT

A novel series of supramolecular hydrogen bonded ferroelectric liquid crystal (HBFLC) is formed through hydrogen bonding interaction between nonmesogenic dextro-levo tartaric acid (DLTA) and mesogenic p-n-alkyloxy benzoic acids (nBAO, where n = 7 to 12). The formation of hydrogen bond in the complex is confirmed through Fourier transform infrared spectroscopy (FTIR) studies. Optical and thermal behaviors for mesomorphic phases of individual complex in the series are meticulously studied by means of differential scanning calorimetry (DSC) and polarizing optical microscopy (POM). Computation of the enthalpy values in the homologous series of complex during both heating and cooling cycles is proved that thermal equilibrium exhibited by the complex system. Extended thermal span width and rich liquid crystallinity is observed in the present complex due to the presence of aromatic ring with chiral center. Thermal stability factor and thermal equilibrium are also discussed. Presence of alkyloxy chain on either side of chiral molecules hinder the abundant reduction in phase transition temperature and lowered melting point compared to the individual mesogens. Optical tilt angle for smectic C* phase is determined and the same is fitted to a power law.

KEYWORDS

Smectic; POM; DSC; thermal stability factor

1. Introduction

Liquid crystals (LCs) exhibiting the intermediate phases between isotropic liquid and solid crystal during their phase transitions which have both liquid and crystal properties [1]. Molecular orientation and self-assembly systems are the basic requirements for exhibiting these interesting properties. A single LC may not satisfy all the requirements of our day-to-day life applications. Usually, supplement/compliment properties of multicomponent LC mixture is more useful for industrial applications. In particular more than two LCs are mixed with each other in definite molar ratio, it gives major effect on intermolecular hydrogen bonding and results in diversity of thermodynamic and optical properties [2–4]. In the recent decade, various research groups all around the world interesting to work on the synthesis of liquid crystal complexes through intermolecular hydrogen bonding [5–7]. The variety

CONTACT V. N. Vijayakumar vnvphysics@gmail.com Department of Physics, Condensed Matter Research Laboratory (CMRL), Bannari Amman Institute of Technology, Sathyamangalam 638 401, India.
Color versions of one or more of the figures in the article can be found online at www.tandfonline.com/gmcl.

of liquid crystal systems induced by the intermolecular hydrogen bonding was investigated [8]. The first compounds which exhibit liquid crystalline behavior due to hydrogen bond formation were aromatic carboxylic acids [9].

These compounds dimerize through hydrogen bonds leading to a lengthening of the rigid-rod moiety, which in sequence induces liquid crystallinity. The design of hydrogen bonded liquid crystals (HBLCs) with noncovalent interactions through hydrogen bonding made attention towards the synthesis of self-assembly systems [10, 11]. The HBLCs are synthesized from different materials on the basis of their molecular reorganization and self-assembly capabilities [12–14, 15].

Due to HBLC's capability to stabilize the LC phases through hydrogen bonding, most of researchers are interested in working in the field of display devices [8, 16–19]. In addition, the LC phase stability in the mesogens depends on factors such as nature of chemical moieties, composition of mixture and geometry of molecular structure [20, 21]. The characteristic studies on mesophase stability in linear HBLCs such as interaction of substitute atom with electro negativity and their induced mesomorphism were reported [22, 23]. Self-assembly progression via formation of intermolecular interactions in H-bonding is a potential material for the invention of new functional materials [24]. Existing dimeric form of *p-n*-alkoxybenzoic acids and their mixtures is a challenging material to produce an LCs with conventional properties. This dimeric generates molecule may drastically influence the interesting properties of LC materials [25]. Supra molecular HBFLCs provide opportunities to design, synthesis and characterize the various new chemical combinations. Binary mixtures can be synthesized in such a way so as to elevate the desirable thermal span of a specified phase. Many such studies on binary mixtures in the literatures are reported [26–30].

The composition of chemical moieties and length of flexible chain are found to be effect on the mesophases stability in ternary systems of HBLCs [31].The self-assembly systems formed between alkyl and alkyloxy carboxylic acids [32–34] which exhibit rich polymorphism and induce variety of new phenomena like, re-entrant phase occurrence, light modulation, optical shuttering action and field induced transitions. In present research work, DLTA which is nonmesogenic nature and nBAO (n = 7 to 12) mesogenic nature are selected as the chemical moiety ingredients to design the HBFLCs.

2. Experimental

2.1. Materials and methods

Dextro-Levo tartaric acid (DLTA), p-n-alkylocyloxy benzoic acid (nBAO where n = 7 to 12) were supplied by Sigma Aldrich, Germany and all the solvents used were E.Merck grade. The liquid crystal (LC) sample is filled in its isotropic state to a homogenous alignment LC cell which are commercially available (Instec, USA) of 5 × 5 mm^2 indium tin oxide coated area with 4 μm spacer by capillary action and it is subjected to heating followed by cooling scan.

This LC cell is placed in a hot stage MHCS400 (MicrOptik) where the temperature is monitored by a MTDC600 temperature controller (MicrOptik) which is interfaced with a computer and controlled by a software program to a temperature resolution of ± 0.1°C. The hot stage is placed under crossed polarizer of Ningbo polarizing microscope for optical textural studies equipped with digital unit (ToupTek). Optical images of mesogens are captured using a Sony CCD.17.UH310 USB CCD 3.1MP camera during heating and cooling scan at the rate of 1°C min^{-1} and the same are analyzed by using software.

Shimadzu DSC60 Plus with Ta60 software (version 2.21) and TAC-60i mechanical auto-cooling system is used for obtaining transition temperatures and enthalpy values of mesogens. 4g Mass of the DLTA: nBAO homologous series/ HBFLC were accurately weighed by using a Shimadzu microbalance. The weighed DLTA: nBAO complexes are sealed in aluminum pans separately and they are heated (at the rate of 5°C min^{-1}) up to a temperature above the estimated clearing temperature and hold at its isotropic temperature for two minutes so as to attain thermal stability. Once a stable heat flow is sustained, the samples are cooled at a rate of 5°C min^{-1} to 30°C. All DSC curves are corrected using baselines recorded under identical conditions. FTIR spectra are recorded (ABB FTIR MB3000) by making pellet of the DLTA: nBAO homologous series are analyzed using the MB3000 software to identify the formation of H-bond in the DLTA: nBAO homologous series.

2.2. Synthesis of HBFLC complexes

The dimerization is usually depends on the surrounding conditions like temperature and external stimulus. Therefore the existing dimeric form of p-n- alkyloxy benzoic acid (nBAO) is converted to monomeric form by using excess tetrahydrofuran (THF) as depicted in Scheme 1. Initially nBAO is dissolved in excess THF and stirred 12 hours with 750 rpm using magnetic stirrer to obtain white crystalline complex. For the preparation of the HBFLC mixtures, the DLTA and nBAO (n = 6 to 12) monomer homologous were taken in 1:2 molar ratio, respectively. Then the same is kept in silicon oil bath by melting the appropriated amounts of each compound above their clearing point and then slowly cooling (3 to 5 hours) to room temperature as shown in Scheme 2. The white crystalline complex was obtained as an end product. The molecular structure of isolated double HBFLC complexes from dextro-levo tartaric acid and p-n-alkyloxy benzoic acids is depicted in Scheme 2.

3. Result and discussion

3.1. FTIR studies

Intermolecular hydrogen bonding between the chemical moieties could be resolved using the FTIR spectra. From the absorption of various frequencies of electromagnetic radiation in the infrared region by the chemical substance the covalent bonds can be easily identified. Thus, the absorption of infrared gives rise to various energy transactions. So the bond formation and the types of stretching can be inferred from it. Only the bonds having dipole moment that change as a function of time are capable of absorption of infrared radiation. So FTIR spectrum

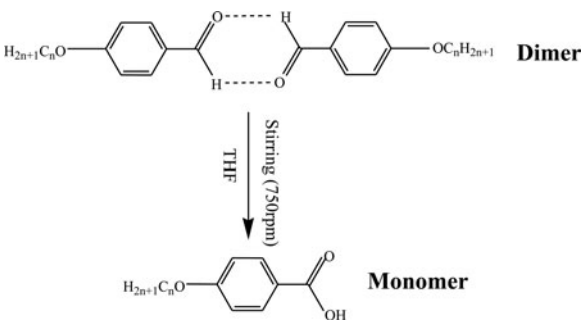

Scheme 1. Synthesis of monomer.

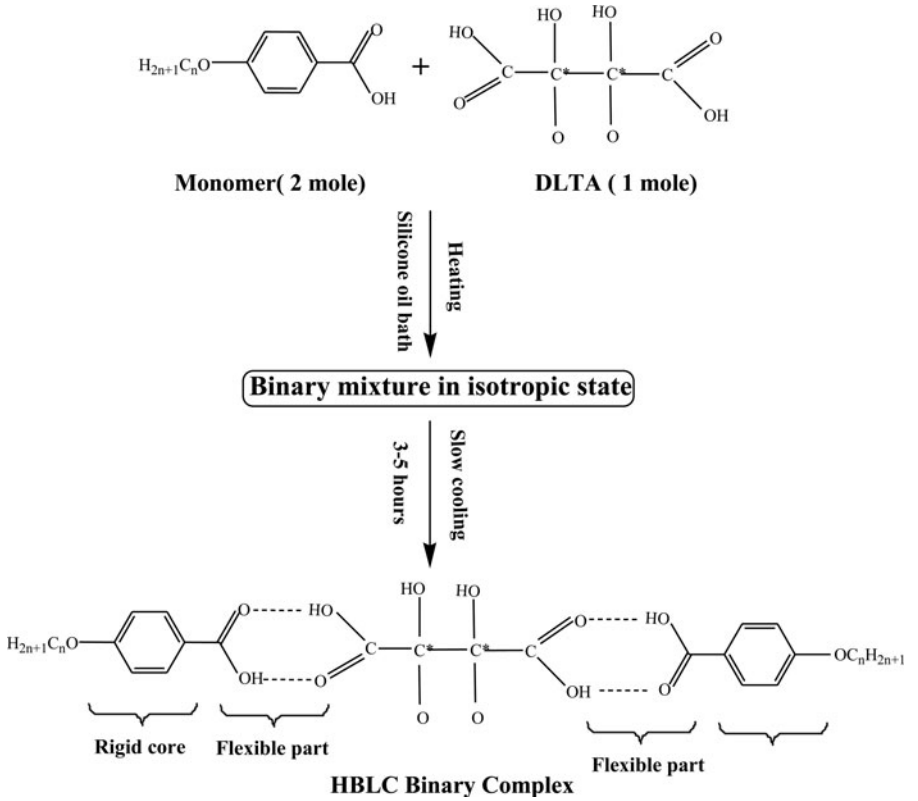

Scheme 2. Synthesis of DLTA + nBAO HBLC.

can be used to identify the molecular environment chemical moieties. In the present HBFLC complex, the formation of hydrogen bond in DLTA + 9BAO is confirmed through FTIR studies as inter-molecular, double, alternative and complementary type (Figure 1). Vibrational spectral assignment of stretching mode in the bond formation is recorded for whole homologues series of binary complex in the solid state (KBr) at room temperature to identify

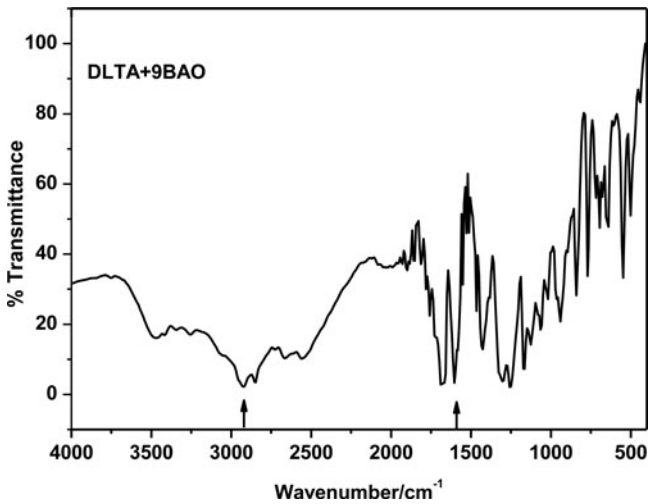

Figure 1. FTIR spectrum of DLTA + 9BAO HBLC.

Table 1. FTIR peak values for homologues series of DLTA + nBAO complexes.

	Stretching modes in DLTA + nBAOs (cm^{-1})	
Complexes	γ(O–H)	γ(C=O)
DLTA with 7BAO	2856	1689
DLTA with 8BAO	2854	1690
DLTA with 9BAO	2846	1690
DLTA with 10BAO	2857	1689
DLTA with 11BAO	2854	1691
DLTA with 12BAO	2852	1692

the presence of intermolecular hydrogen bonding and the same is depicted in Table 1. As a representative case, the FTIR result for HBFLC complex of DLTA and 4-nonyloxy benzoic acid (9BAO) is discussed for the formation of H-bond in the molecular structure. In IR spectrum, monomeric form of nBAO exhibits two peak assignments at due to ν(—C═O) stretching vibrations owing to ν(—C═O) stretching vibrations reported [35–37]. The bands corresponding to carbonyl group have been subjected to extensive studies [38] because of its vibrations give rise to characteristic bands in vibrational spectra. The formation of hydrogen bond increases the intensity of these bands. It is reported [39] that carbonyl stretching vibrations in the monomeric mesogens were occurred at peaks corresponding to 1685 and 1695 cm^{-1}. Results in the electron donating, dimer formation can be formed by introducing the hydrogen bond in the complex. In the present study, the peaks associated with C═O stretching bands for (DLTA+9BAO) binary complex were found at 1689 cm^{-1} in FTIR spectrum. This is an evidence for the existence of inter molecular hydrogen bond in the dimer.

Vibrations of O–H bond stretching are responsive to hydrogen bonding. The nonhydrogen bonded or free hydroxyl group absorbs strongly in the peak range from 3600 to 3550 cm^{-1} whereas the presence of an intermolecular hydrogen bonding can have lower wave number region then that of O–H stretching result in increased IR intensity and breadth. In the recorded IR spectrum of (DLTA + 9BAO) binary LC system, a sharp peak at 2954 cm^{-1} represents the existence of –OH stretching which confirms the dimeric nature of hydrogen bonded presented in the binary complex.

3.2. Phase characterization and identification of mesophases by POM

The synthesized HBLC complex is highly stable at ambient temperature (~30°C). HBFLC complexes melt at particular temperature below ~98°C and it shows high thermal and chemical stability when subjected to repeated thermal scans performed by POM and DSC. The textural changes for various mesophases in the complex can be observed through POM when it is kept under crossed polarizer and corresponding results are recorded simultaneously. The observed characteristic textures are compared with reference textures reported in the literature [39]. All complexes in the present homologous series exhibited enantiotropic phase transitions during heating cycle as well as cooling cycle.

The various characteristic textures of the present HBFLC homologous series were observed by associating with reported [40] textures. According to this, present HBFLC complexes exhibited the various mesophases such as threaded nematic texture (N*), Smectic C* (Sm C*) phase with marble threaded texture, Smectic G* (Sm G*) with multi colored mosaic texture as shown in Figure 2. As a representative case, HBFLC complex of dextro- levo tartaric

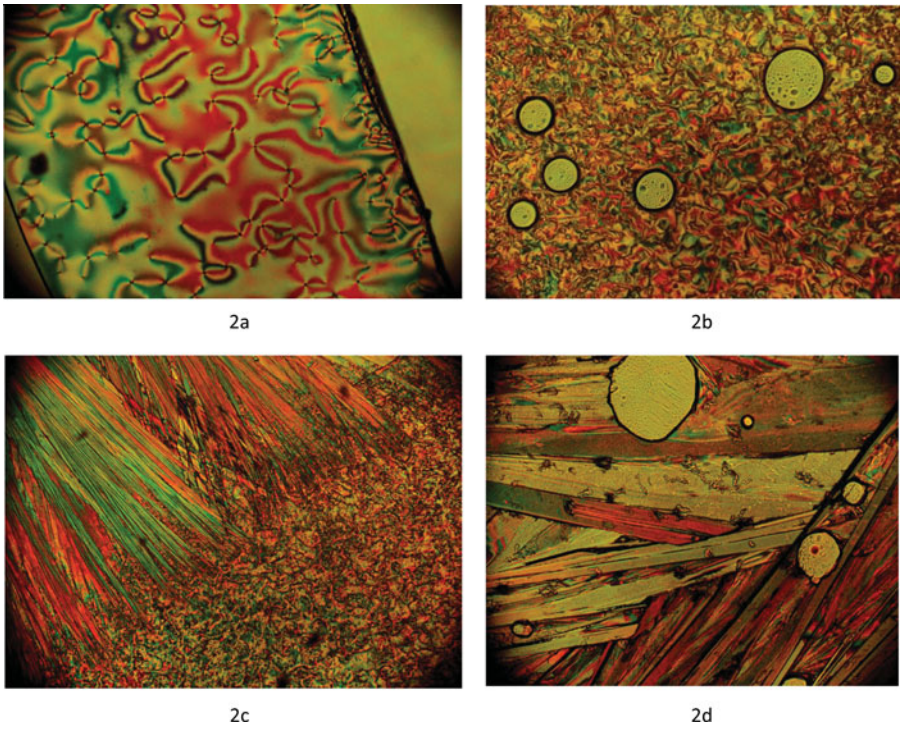

Figure 2. Characteristic textures of mesophases in DLTA + 10BAO HBLC.

acid with octyloxy benzoic acid (DLTA + 10BAO) is discussed. This complex shows threaded nematic texture (N*) phase (132°C), schlieren texture of smectic C* phase (122.4°C), multi colored mosaic texture of smectic G* phase (90.2°C) with defined boundaries texture as shown in Figure 2a, b, and d, respectively. Growing of Sm G* phase from Sm C* phase in DLTA + 10BAO HBFLC complex is depicted in Figure 2c. There is a rich liquid crystallinity is observed in the complex due to the presence of aromatic ring with chiral centre in DLTA + 10BAO HBFLC complex.

An outline of POM observations in DLTA+nBAO homologous series is that H-bond influences marginally in lower homologous considerably in intermediate homologous and rather strongly in higher homologues for the induction of tilted LC phase stability. These observed textures in the present HBFLC complex clearly confirm that the multiple phases are due to the formation of intermolecular H-bond between the non mesogenic chiral complex and mesogenic complex which enable the systematic rearrangement of molecules in the respective mesophases.

The general phase sequences exhibited in the homologous series during cooling scan are represented as

$$\text{Isotropic} \rightarrow \text{N}^* \rightarrow \text{Sm C}^* \rightarrow \text{Sm G}^* \rightarrow \text{Crystal} \quad (\text{DLTA} + \text{nBAO})$$

(where n = 7,8,9,10,11,12).

Table 2. Transition temperatures in centigrade obtained by POM and DSC techniques along with enthalpy values given in J/g.

Compound	Phase Variance	Technique	Cycle	Crystal-Melt	N∗	Sm C∗	Sm G∗	Crystal
(DLTA+7BAO)	N∗C∗G∗	POM	Heating	83.1	148.8	99.3	93.3	
			Cooling		133.9	87.4	86.1	78.6
		DSC	Heating	82.3 (64.71)	147.0 (4.71)	98.4 (1.45)	92.7 (81.71)	
			Cooling		133.0 (2.34)	86.5 (0.41)	85.5 (18.32)	78.4 (25.80)
(DLTA+8BAO)	N∗C∗G∗	POM	Heating	75.3	148.3	108.4	101.5	
			Cooling		134.2	101.8	85.2	55.4
		DSC	Heating	74.4 (36.17)	147.5 (3.77)	107.8 (2.30)	101.1 (25.09)	
			Cooling		133.5 (2.05)	101.1 (0.84)	84.5 (14.83)	54.9 (16.30)
(DLTA+9BAO)	N∗C∗G∗	POM	Heating	67.8	140.8	117.4	93.8	
			Cooling		139.7	106.5	83.7	55.1
		DSC	Heating	66.9 (8.78)	140.0 (0.82)	116.7 (5.98)	93.2 (45.35)	
			Cooling		139.1 (0.38)	105.7 (1.55)	83.2 (4.52)	54.5 (10.71)
(DLTA+10BAO)	N∗C∗G∗	POM	Heating	86.1	142.9	121.6	96.8	
			Cooling		132.7	112.9	90.7	76.5
		DSC	Heating	85.2 (49.62)	142.1 (5.26)	120.9 (3.67)	96.1 (23.95)	
			Cooling		132.0 (3.51)	112.4 (1.39)	90.2 (18.88)	76.0 (12.10)
(DLTA+11BAO)	N∗C∗G∗	POM	Heating	97.4	130.5	117.9	103.8	
			Cooling		130.4	123.5	80.5	71.1
		DSC	Heating	96.4 (108.09)	129.8 (7.94)	117.3 (9.67)	103.2 (0.61)	
			Cooling		129.8 (5.19)	122.9 (8.23)	80.0 (20.97)	70.6 (12.03)
(DLTA+12BAO)	N∗C∗G∗	POM	Heating	95.2	139.1	123.8	#	
			Cooling		132.8	126.1	85.6	59.2
		DSC	Heating	94.3 (94.76)	138.4 (17.67)	132.2 (4.78)	86.3 (10.61)	
			Cooling		132.2 (5.32)	125.4 (3.62)	81.1 (24.65)	58.8 (11.42)

#Monotropic transition.

3.3. DSC studies

From the meticulous observation from DSC curves of the homologous series of DLTA + nBAO during heating and cooling scan for the various phase transitions, we noticed that phase transition from isotropic to N*, N* to Sm C*, Sm C* to Sm G*, and Sm G* to crystal which is found to be identical with respective to thermal span width. The corresponding enthalpy values of all individual phases in the homologous series are given in the Table 2. As chain length increases this favors the enhancement in the thermal range of mesophases. So the enhancement of thermal range in the present complex is due to the H-bond between O and OH group of the two different carboxylic acids.

DSC thermograms for all complexes in the present homologous series are obtained with scan rate of 10°C/min in both heating (Figure 3) and cooling (Figure 4) cycles. The respective equilibrium transition temperatures along with corresponding enthalpy values of mesogens are recorded and the same is presented in Table 1. Transition temperatures obtained from DSC thermogram are well concurrent with those obtained through POM studies. It is noticed (Figure 5) that the thermal span width is decreasing while increasing the alkyloxy carbon number. As shown in Figure 5 the N* phase width is minimum in DLTA+12BAO complex where as the same phase width is maximum in DLTA + 10BAO complex. But the thermal span width of Sm C* shows maximum value (~44°C) in DLTA + 12BAO complex while the same (Figure 6) is minimum (~22°C) in the lower alkyloxy carbon number (DLTA + 10BAO) complex. Similarly Figure 7 reveals that the thermal span width of smectic G* phase is decreased gradually while alkyloxy carbon number increases from 8 to 11. Because of the attachment of alkyloxy chain on either side of chiral molecules, few complex in the series shows abundant reduction in phase transition temperature, lowered melting point compared to the individual mesogen. The melting point reaches its minimum at the eutectic point and

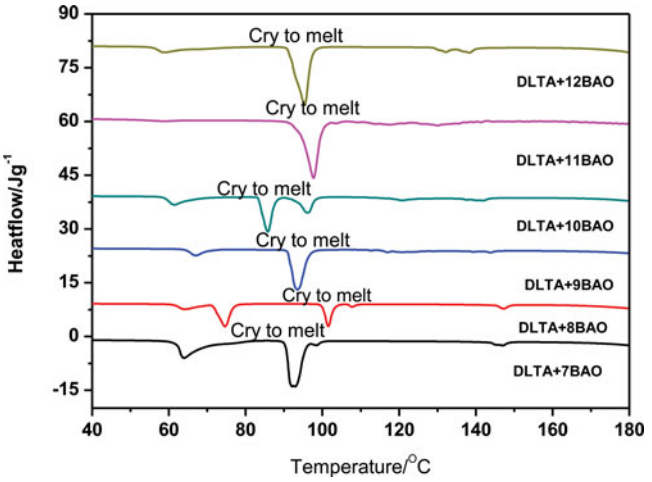

Figure 3. DSC thermogram of DLTA + nBAO HBFLC homologous series during heating cycle.

usually clearing point of the mesogenic complex is the linear average of composition, hence the mesogenic mixture can offer a much wider temperature range that exhibit the smectic C* phase for display applications.

As a representative case, the phase transitions across various mesophases in the DLTA + nBAO series, the DLTA + 10BAO HBLC along with their transition temperature and enthalpy values are discussed. The DSC thermogram of DLTA + 10BAO complex is recorded in both heating and cooling cycle at a scan rate of 10°C/min is shown in Figure 8. From the thermogram, it was observed the four characteristic phase transitions from isotropic to N*, N* to Sm C*, Sm C* to Sm G* and Sm G* to crystal with transition temperature at 132.0°C, 112.4°C, 90.2°C, 76.0°C and corresponding enthalpy values are 3.51 J/g, 1.39 J/g, 18.88 J/g and 12.10 J/g, respectively. Also in heating cycle, four distant transitions were identified from crystal to melt, melt to Sm G*, Sm G* to Sm C*, and Sm C* to N * at 85.2°C, 96.1°C, 120.9°C, and 142.1°C with corresponding enthalpy values of 49.62 J/g, 5.26 J/g, 3.67 J/g, and 23.95 J/g,

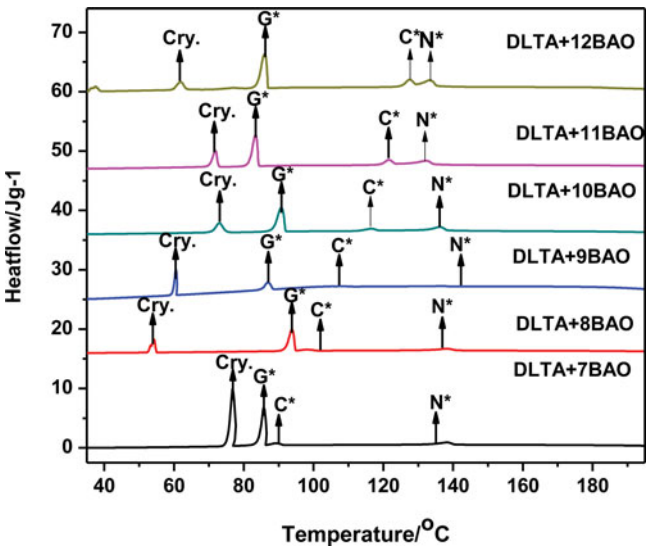

Figure 4. DSC thermogram of DLTA + nBAO HBFLC homologous series during cooling cycle.

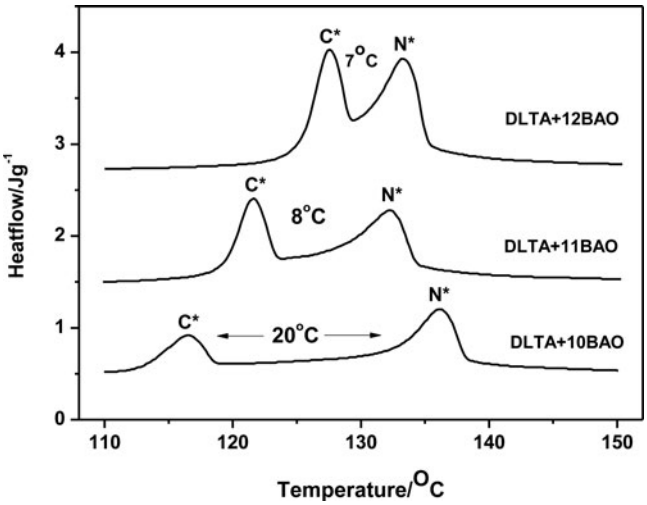

Figure 5. DSC thermogram of N* to Sm C*phase transition in DLTA + nBAO HBFLC homologous series.

respectively. All transition temperatures of various mesophases in the homologous series were in accord with POM observations.

3.4. Phase diagram of DLTA: nBAO homologues series

The phase diagram for present homologous series is drawn from the temperature parameters obtained through the DSC studies. The phase variance of nBAO is occurred across various mesophases like nematic (N), Sm C, and Sm G reported [40].

Since DLTA is nonmesogenic nature, it does not have any mesophase, whereas alkyloxy benzoic acids are mesogenic nature. The homologous series of HBLC complexes were obtained from DLTA with nBAO associated with alkyloxy carbon number from 7 to 12, they exhibited rich phase polymorphism as reported by earlier [39]. Six complexes in the homologous series of DLTA + nBAO were studied. The changes of phase behaviours in the series were discussed through phase diagram drawn between phase transition temperatures and alkyloxy

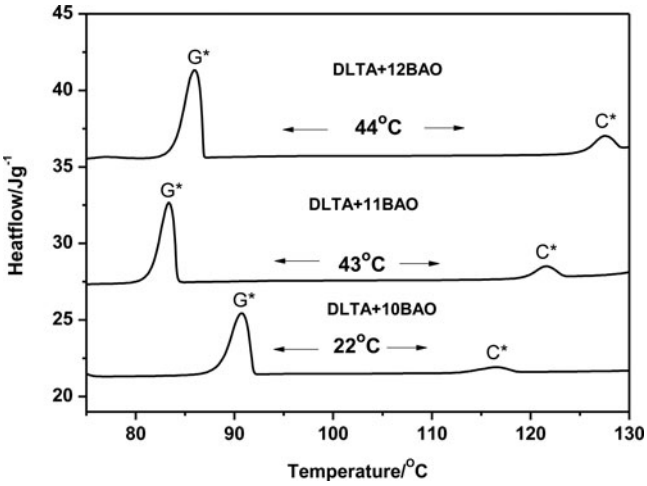

Figure 6. DSC thermogram of Sm C* to Sm G*phase transition in DLTA + nBAO HBFLC homologous series.

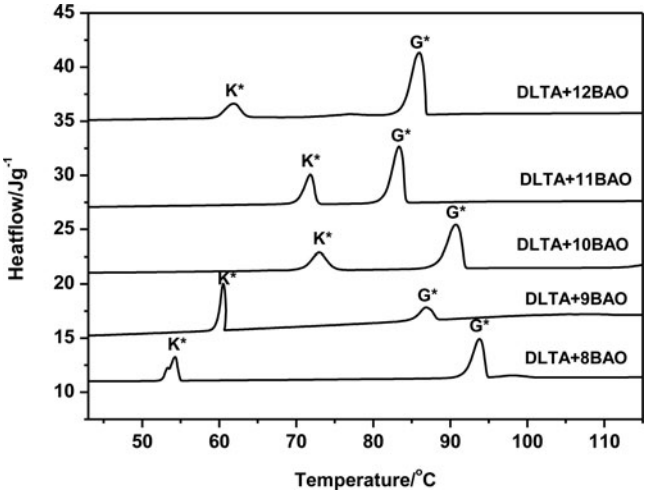

Figure 7. DSC thermogram of Sm G* to crystal phase transition in DLTA + nBAO HBFLC homologous series.

carbon numbers as shown in Figure 9. From phase diagram, the following conclusions are made:

(a) All complexes in the series composed of three mesophases namely N*, Sm C*, and Sm G*. Due to the formation of H-bond between mesogenic and nonmesogenic in the present HBFLC complex induce rich phase polymorphism.
(b) The lower homologous in DLTA + nBAO HBFLC shows induced highly ordered Sm G* whereas same is not observed in the its constituent compounds
(c) It is interesting to note that all complexes in the DLTA + nOBA series exhibit all the four phases (N*C*G*), while pure nBAO (n = 7 to 9) possess two phases namely, nematic and smectic C.
(d) The lower homologous exhibit N* phase with high thermal span but the N* quenching while increasing alkyloxy carbon number in the DLTA+nBAO HBFLC series. At the same time Sm G* shows anomalous behaviour.
(e) In contrast, the Sm C* phase width increases while increasing alkyloxy carbon number.

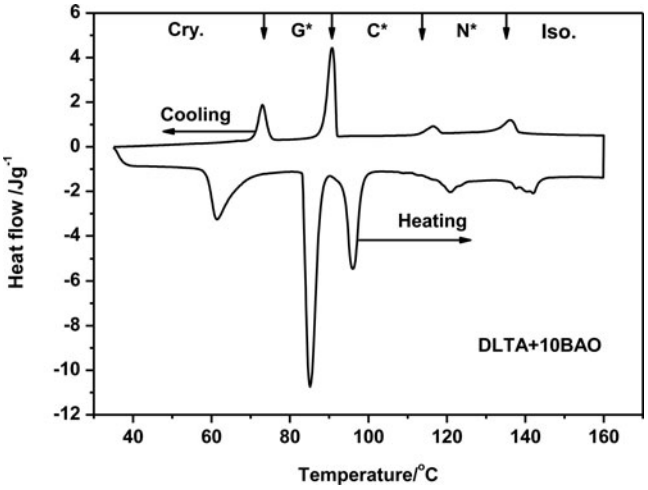

Figure 8. DSC thermogram of DLTA+10BAO HBFLC complex.

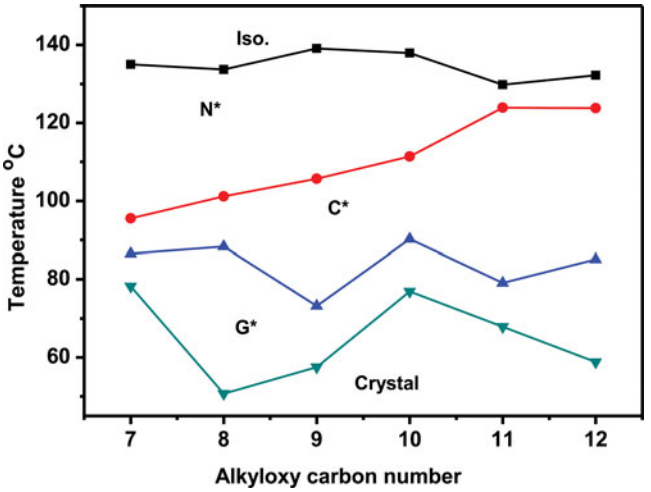

Figure 9. Stability factor for DLTA + nBAO HBFLC homologous series.

(f) Similarly, odd-even effect is predominated in the SmC* to Sm G* and Sm G* to crystal transitions over to other transitions.
(g) The lower homologous show higher clearing point than the higher homologous.
(h) In general, DLTA + 7BAO HBFLC show the smallest mesogenic thermal range of ~54.6°C while DLTA + 9BAO HBFLC mesogen has the largest mesogenic thermal range of ~85°C.

3.5. Thermal stability factor

It is an important parameter to estimate the benefits of LC materials for device applications. It also strongly depends on the molecular structure of the complex such as, flexible core and rigid core of the alkyloxy chain length. Normally liquid crystalline molecules have two symmetric end chains, the phase transition temperatures and the thermal span ranges are affected [41, 42]. The molecular weights of terminal chain could be considered as the measure of balancing, and if they are nearly equal, the system is balanced. In other words, the system is symmetric about its molecular short axis.

Phase stability is one of the essential parameters that govern the utility of the mesogen. As a representative case, phase stability of Sm C* for DLTA+9BAO complex is discussed. The term phase stability can be attributed to N* to Sm C* transition temperature as well to the temperature range of Sm C* phase. It is reasonable to consider both the above factors and define a parameter called thermal stability factor (S).The stability factor for Sm C* phase is

$$S_{C*} = T_{\text{mid}} \times \Delta T_{C*}$$

where T_{mid} is the mid Sm C* temperature with respect to nematic N* phase, and ΔT_{C^*} is the Sm C* thermal range. The thermal stability of Sm C* exhibited by DLTA + 9BAO complex is calculated as 2125. By following the same procedure the thermal stability of other phases for remaining complexes in the present homologous series are calculated and the same is appended in Table 3. The variation of stability factors with respect to alkyloxy carbon numbers for the present homologous series is explained (Figure 10). It has been observed that stability factor values increase with increase the carbon numbers and the combination in the LC mixture alters the thermal stability of the phases with respect to their thermal span. In

Table 3. Thermal stability factor for DLTA : nBAO homologous series in different phases.

HBFLC complex	N*	Sm C*	Sm G*
DLTA + 7BAO	5103.38	86.00	25.21
DLTA + 8BAO	3800.52	1540.48	438.08
DLTA + 9BAO	4088.16	2125.13	411.85
DLTA + 10BAO	2395.12	2248.86	100.82
DLTA + 11BAO	871.82	4352.21	44.18
DLTA + 12BAO	875.84	4241.58	345.85

particular, the thermal stability factor in Sm C* phase has maximum value in its higher alkyloxy carbon number where as very low in its lower counter parts. This clearly shows that the reorientation of the molecules with respect to director during the different phase transitions of the HBFLC complex occurs at systematic foundations.

3.6. Optical tilt angle studies

The angle inclined between direction of aligned molecules along optic axis and reference axis is said to be optical tilt angle. The location of molecules in mesophase with reference coordinate system in mesogenic complex depends on tilt angle. To explain this, the direction vertical to the layer plane in smectic phase is considered as reference axis.

The tilt angle of smectic C* phase in given mesogenic complex is experimentally evaluated by optical extinction method [43, 44].The changes in temperature is determined by applying the measured data of temperature $\theta\ (T)$ in relation given below,

$$\theta\ (T)\,\alpha\,\theta_0(T - T_c)^{\beta}$$

where $\theta\ (T)$ is temperature at which tilt is taken (°C), T is temperature (°C), T_c is phase transition temperature (°C), θ_0 is a arbitrary constant and β is critical exponent value which is determined by fitting temperature data to the above expression and it is found to be 0.50 which is well agreement with the mean field value prediction [45].

Optical tilt angle has been experimentally determined in the smectic C* phase of DLTA + nBAO complex and the same is given in Table 4. From the Figure 11, it is found that the tilt angle is increases with decreasing temperature and reaches a saturation value. For tilt angle

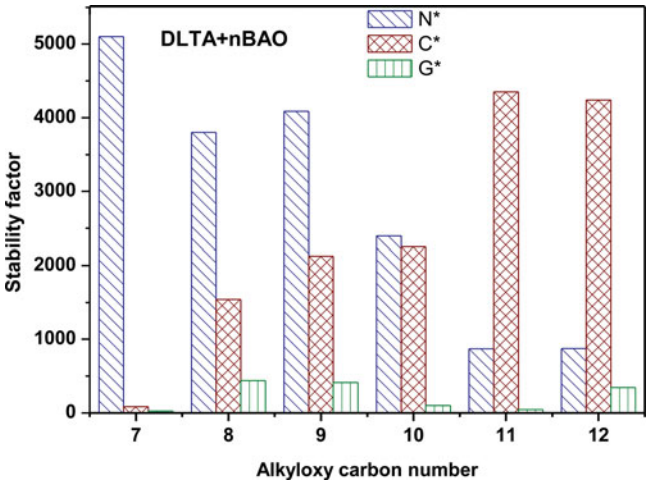

Figure 10. Phase diagram of DLTA + nBAO HBFLC series.

Table 4. Maximum tilt angle for Smectic C* in DLTA : nBAO HBLC complex.

HBFLC complex	Tilt angle value
DLTA + 7BAO	15
DLTA + 8BAO	15
DLTA + 9BAO	16
DLTA + 10BAO	17
DLTA + 11BAO	18
DLTA + 12BAO	18

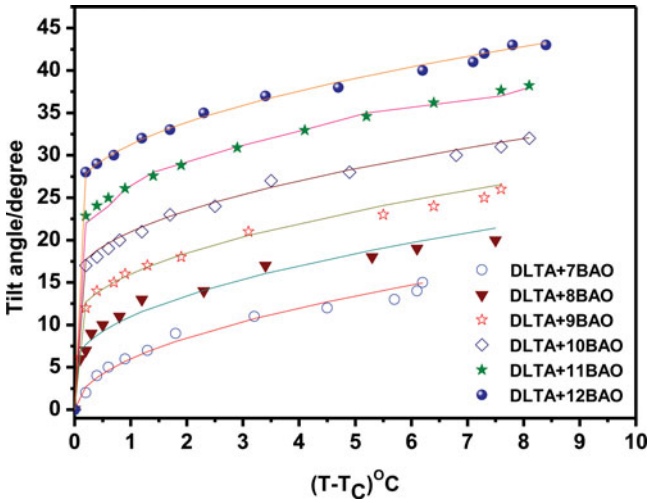

Figure 11. Tilt angle measurements for DLTA + nBAO HBFLC series.

in smectic C*, the saturated value is found to be maximum 18° at DLTA+12BAO HBFLC complex. This saturated value is attributed to the direction of soft covalent hydrogen bond interaction which lengthens along the molecular axis with finite inclination. The dotted line in the graph indicates fitted data. The agreement of β value with mean field value depicts the long range interaction of transverse dipole moment for the stabilization of titled smectic C phase.

4. Conclusion

The characteristic textures and their corresponding transition temperatures along with enthalpy values are analyzed in the homologous series of DLTA + nBAO HBFLC complex by POM and DSC studies, respectively. The presence of H-bond and tilted chiral phases are evinced through FTIR and tilt angle measurement studies. A note worthy observation is that an induced Sm G* is observed in the present homologues series. The lowering of melting point and clearing point of individual complexes are discussed along with increased thermal span of different mesophases. The phase behaviour studies of various HBFLC complexes in DLTA + nBAO homologous series is discussed.

Acknowledgments

The author (V N Vijayakumar) acknowledges the financial support rendered by Department of Science and Technology (No.SERB/F/7454/2013–2014 dated 21.02.2014), New Delhi and Department of Atomic Energy (No: 34/14/14/2016-BRNS/34039 dated 22/04/2016) – Board of Research in

Nuclear Science (DAE-BRNS) and infrastructural support provided by Bannari Amman Institute of Technology.

References

[1] Chandrasekhar, S. (1992). *Liquid Crystals*, 2nd Ed., University Press: Cambridge.
[2] Diele, S., Pelzl, G., Weissflog, W., & Demus, D. (1988). *Liq. Cryst.*, *3*, 1047–1053.
[3] Jaishi, B. R., Mandal, P. K., & Dabrowski, R. (2010). *Opto-Electron Rev.*, *18*, 111–120.
[4] Sridevi, B., Chalapathi, P. V., Srinivasulu, M., Pisipati, V. G. K. M., & Potukuchi, D. M. (2004). *Liq. Cryst.*, *31*, 303.
[5] Martinez-Felipe, A., & Imrie, C. T. (2015). *J. Mol. Struct.*, *1100*, 429–437.
[6] Jansze, S. M., Martinez-Felipe, A., Storey, J. M. D., Marcelis, A. T. M., & Imrie, C. T. (2015). *54*, 643–646.
[7] Paterson, D. A., Martinez-Felipe, A., Jansze, S. M., Marcelis, A. T. M., Storey, J. M. D. et al. (2015). *Liq. Cryst.*, *42*, 928–939.
[8] Kato, T., & Frechet, J. M. J. (1989). *J. Am. Chem. Soc.*, *111*, 8533–8534.
[9] Singh, S. (2008). Liquid Crystals; Fundamentals, World Scientific: London.
[10] Kelker, H., & Hats, R. (1980). Handbook of Liquid Crystals, Verlag Chemie: Weinheim, Germany.
[11] Parra, M., Hidalgo, P., & Alderete, J. (2005). *Liq. Cryst.*, *32*, 449–455.
[12] Kato, T., & Frechet, J. M. J. (1995). *Macromol. Symp.*, *95*, 311–326.
[13] Kato, T., Nakano, M., Moteki, T., Uryu, T., & Ujiie, S. (1995). *Macromolecules*, *28*, 8875–8876.
[14] Kato, T. (1996). *Supra. Mol.Sci.*, *3*, 53–59.
[15] Alfonso, M. F., & Imrie, C. T. (2015). *J. Mol. Struc.*, *1100*, 429–437.
[16] Lehn, J. M. (2002). Toward self organization and complexes. *Meter. Sci.*, *295*, 2400–2003.
[17] Prins, J., Reinhoudt, D. N., & Timmerman, P. (2001). *Angew. Chem.*, *113*, 2446–2492.
[18] Bhagavath, P., Mahabaleshwara, S., Sangeetha, G., Potukuchi, D. M., Chalapathi, P. V. et al. (2013). *J. Mol. Liq.*, *186*, 56–62.
[19] Muni Prasad, M., Madhu Mohan, M. L. N., Chalapathi, P. V., Ashok Kumar, A. V. N., & Potukuchi, D. M. (2015). *J. Mol. Liq.*, *207*, 294–308.
[20] Luckhurst, G. R., & Gray, G. W. (1979). The Molecular Physics of Liquid Crystals, Academic Press: New York.
[21] Kato, T., Kihara, H., Uryu, T., Fujishima, A., & Frechet, J. M. J. (1992). *Macromolecules*, *25*, 6836–6841.
[22] Bhagavath, P., Bhat, S. G., Mahabaleshwara, S., Girish, S. R., Potukuchi, D. M. et al. (2013). *J. Mol. Struct.*, *1039*, 94–100.
[23] Rambabu, M., Prasad, K. R. S., Venu Gopala Rao, M., Madhav, B. T. P., & Pisipati, V. G. K. M. (2015). *Liq. Cryst.*, *24*, 81–92.
[24] Kalinin, N. V., Emelyanenko, A. V., Nosikova, L. A., & Kudryashova, Z. A. (2013). *Phys. Rev.*, *E87*, 062502.
[25] Efremova, E. I., Kydryashova, Z. A., Nosikova, L. A., Kovshik, A. P., Dobrun, L. A. et al. (2016). *Mol. Cryst. Liq. Cryst.*, *626*, 12–20.
[26] Okumuş, M. (2015). *J. Therm. Anal. Calorim.*, *120*, 1603–1608.
[27] George, A. K., Potukuchi, D. M., Al-Harthi, S. H., & Carboni, C. (2004). *Z.Naturforsch*, *59*, 659–664.
[28] Kato, T., & Frechet, J. M. J. (1989). *J. Am. Chem. Soc.*, *111*, 8533–8534.
[29] Pongali Sathya Prabhu, N., & Madhu Mohan, M. L. N. (2012). *Mol. Cryst. Liq. Cryst.*, *562*, 177–190.
[30] Kumar, S. (2010). Chemistry of Discotic Liquid Crystals: From Monomer to Polymer, CRC Press: Florida.
[31] Okumuş, M., & Özgan, Ş. (2014). *Liq. Cryst.*, *41*, 1293–1302.
[32] Mahalingam, T., Venkatachalam, T., Jayaprakasam, R., & Vijayakumar. V. N. (2016). *Braz. J. Phys.*, *46*(3), 273–281, DOI 10.1007/s13538-016-0415-6
[33] Vijayakumar, V. N., & Madhu Mohan, M. L. N. (2010). *Solid State Sci.*, *12*, 482–489.
[34] Vijayakumar, V. N., & Madhu Mohan, M. L. N. (2011). *J. Mol. Struct.*, *991*, 60–67.
[35] Kato, T., Uryu, T., Kaneuchi, F., Jin, C., & Fréchet, J. M. J. (1993). *Liq. Cryst.*, *14*, 1311–1317.
[36] Nakamoto, K. (1978). Infrared and Raman Spectra of Inorganic and Co-Ordination Compounds. 4th Ed., Interscience: New York.

[37] Mitsuo, T. (2015). Introduction to Experimental Infrared Spectroscopy: Fundamentals and Practical Methods. 1st Ed; John Wiley and Sons Ltd: United Kingdom.
[38] Eusebio, S., Sebastião, P. J., & Manuela. R. S. (2014). *Liq. Cryst.*, *41*, 1743–1751.
[39] Gray, G. W., & Goodby, J. W. (1984). Smectic Liquid Crystals – Textures and Structures, Leonard Hill: London.
[40] Vijayakumar, V. N., Murugadass, K., & Madhu Mohan, M. L. N. (2010). *Mol. Cryst. Liq. Cryst.*, *517*, 41–60.
[41] Smith, G. W., & Gardlund, Z. G. (1973). *J. Chem. Phys.*, *596*, 3214–3228.
[42] Osman, Z. (1976). *Z. Naturforsch.*, *31*, 801–804.
[43] John, D., & Saupe, A. (1977). *Phys. Rev. Lett.*, 152079–2085.
[44] Taylor, T. A., Fergason, J. L., & Arora, S. L. (1970). *Phys. Rev. Lett.*, *24*, 359–362.
[45] Stanley, H. E. (1971). Introduction to Phase Transition and Critical Phenomena, Oxford University Press, UK.